Available online at www.sciencedirect.com
SCIENCE DIRECT®
Biochemical Pharmacology 68 (2004) 1443–1452
Biochemical Pharmacology
www.elsevier.com/locate/biochempharm

Dynamics of interactions of photosensitizers with lipoproteins and membrane-models: correlation with cellular incorporation and subcellular distribution

Stéphanie Bonneau[a], Patrice Morlière[b], Daniel Brault[a,*]

[a]*Laboratoire de Physicochimie Biomoléculaire et Cellulaire, Université Pierre et Marie Curie, CNRS UMR 7033, 75005 Paris, France*
[b]*INSERM U532, Laboratoire de Photobiologie, Muséum National d'Histoire Naturelle, 75005 Paris, France*

Received 1 March 2004; accepted 17 June 2004

Abstract

The incorporation and subcellular localization of photosensitizers are critical determinants of their efficiency. Here, we correlate these properties with the interactions of photosensitizers with membrane-models and low density lipoproteins (LDL) in acellular systems. Focus was given on dynamics aspects. Two amphiphilic photosensitizers, deuteroporphyrin (DP) and aluminum phthalocyanine sulfonated on two adjacent isoindole units (AlPcS2a) were selected. The phthalocyanine was bound to LDL with an overall association constant around $5 \times 10^7\ M^{-1}$. Biphasic association kinetics was indicative of two types of sites. The release of the phthalocyanine into the bulk aqueous medium occurred within less than a second. A similar behavior was found previously for deuteroporphyrin although its affinity was somewhat higher ($5.5 \times 10^8\ M^{-1}$). Both compounds were previously characterized by high affinity for membrane-models and quick exchange with the bulk solution. However, they strongly differed by their rate of transfer through the lipid bilayer, in the range of seconds for the porphyrin, several hours for the phthalocyanine. In the case of the porphyrin, fluorescence microscopy on human fibroblasts showed diffuse labeling with no significant modification of the distribution upon vectorization by LDL. In contrast, the phthalocyanine was localized in intracellular vesicles. Vectorization by LDL favored lysosomal localization although little effect was found on the overall uptake as shown by extraction experiments. The role of lipoproteins in the cellular localization of photosensitizers is significantly more important for photosensitizers not freely diffusing through bilayers. The dynamics of the interactions of photosensitizers with membranes appears as an important determinant of their subcellular localization.

Keywords: Photosensitizer; Cellular uptake; Lipoprotein; Passive transport; Dynamics; Fluorescence microscopy

1. Introduction

Photodynamic therapy (PDT) is a promising treatment for various oncologic and ophthalmic diseases [1,2]. PDT is based on the light activation of photosensitizers that are retained to some extent by proliferating tissues allowing the formation of a concentration gradient against normal adjacent tissues [3]. Photodynamic therapy involves a systemic administration of the photosensitizer to the patient followed by light irradiation of the targeted tissue after a suitable interval of time. A dual selectivity arises from the drug retention and from the possibility to delineate the zone of light irradiation. As the deleterious toxins produced by light irradiation are very short lived species with a limited diffusion, primary molecular damages affect only subcellular structures labeled by the photosensitizer. Thus, the intracellular distribution of photosensitizers is a major determinant of the primary events although the overall response to those initial damages involves complex cellular pathways [4]. As a matter of fact, the localization of photosensitizers in different organelles or other subcellular structures is well correlated with their overall phototoxicity [5] and the mechanism of cell death [6–8].

The relative photosensitization efficiency and intracellular localization of photosensitizers strongly depend on their structure, in particular on their hydrophobicity and the

Abbreviations: AlPcS2a, disulfonated aluminum phthalocyanine; cps, count per second; DP, deuteroporphyrin; HBSS, Hank's balanced salt solution; LDL, low density lipoproteins; PBS, phosphate buffer saline; PDT, photodynamic therapy.

* Corresponding author. Tel.: +33 1 40 79 36 97; fax: +33 1 40 79 37 16.
E-mail address: brault@mnhn.fr (D. Brault).

0006-2952/$ – see front matter © 2004 Elsevier Inc. All rights reserved.
doi:10.1016/j.bcp.2004.06.014

symmetry of distribution of their polar and hydrophobic chains around the macrocycle [9–11]. The electric charge of the side-chains plays an important role [12]. Two major processes could account for the enhanced retention of certain photosensitizers by proliferating tissues. On one hand, lipophilic or amphiphilic photosensitizers possess a high affinity for low-density lipoproteins (LDL). The increased cholesterol catabolism of proliferating tissues results in over-expression of LDL receptors [13,14]. Hence, LDL could act as natural carriers of photosensitizers and insure their targeting to tumor cells [15–18]. However, the role of LDL has been questioned [19]. On the other hand, the tumor microenvironment, in particular the relative acid pH of extracellular medium could play an important role by governing the physico-chemical properties of photosensitizers. For instance, neutralization of the negative charges of molecules bearing carboxylic chains at lower pH strongly increases their lipophilicity [20,21]. Photofrin®, a preparation made of porphyrin dimers and oligomers that received the first approval for tumor treatment belongs to this category. Thus, a gradient of pH between bulk and intracellular aqueous phases could favor the penetration of this class of photosensitizes within cells [22–24].

The present work aims to correlate the subcellular localization of photosensitizers with their affinity for membranes and LDL and, more importantly, with the dynamics of these interactions. As most of these processes are rapid, we privilege a relatively short incubation time of the cells with the photosensitizer. Focus is given on two amphiphilic photosensitizers: deuteroporphyrin (DP) and disulfonated aluminum phthalocyanine with sulfonate groups on adjacent isoindole units (AlPcS2a). Their structures are given in Fig. 1. DP, a dicarboxylic porphyrin, can be considered as the archetype of Photofrin® components. AlPcS2a is a second-generation photosensitizer with interesting photodynamic properties [25,26]. These two amphiphilic molecules are characterized by an asymmetrical distribution of the polar groups around the macrocycle. They strongly differ, however, by the possibility of neutralization of the negative charges carried by their side-chains and their ability to cross membrane barriers.

2. Materials and methods

2.1. Chemicals

All the physico-chemical experiments were performed in pH 7.4 phosphate buffer saline (PBS). DP was prepared as described previously [20]. Its purity was determined to be better than 99% by HPLC. A stock solution (10^{-3} M) was prepared in distilled tetrahydrofuran (THF) and kept at −18 °C. Experimental solutions were obtained by evaporating an aliquot of the stock solution to make a film that was dissolved in PBS. They were used without delay and renewed frequently. This procedure was found to minimize aggregation and adsorption of DP on glass. The porphyrin solutions were handled in the dark to avoid any photobleaching. Disulfonated aluminium phthalocyanine was kindly furnished by David Phillips (Imperial College of Science, London). It was prepared and characterized as described elsewhere [27,28]. The *cis*-isomer with sulfonated groups on adjacent isoindole units (AlPcS2a) was used. It consists of the α-, α- di-substituted regioisomer that was isolated using reverse phase HPLC. Its structure is shown in Fig. 1b. Human low-density lipoproteins (LDL) were purchased from Calbiochem (San Diego, CA, USA). The material was conditioned at a concentration of 9.62 mg/ml (protein content) in 150 mM NaCl pH 7.4 aqueous solution added with 0.01% EDTA.

2.2. Steady state interactions

Emission spectra were measured using an AMINCO-Bowman 2 spectrofluorimeter (Edison, NJ) equipped with a xenon arc lamp. Recording was generally started 2 min

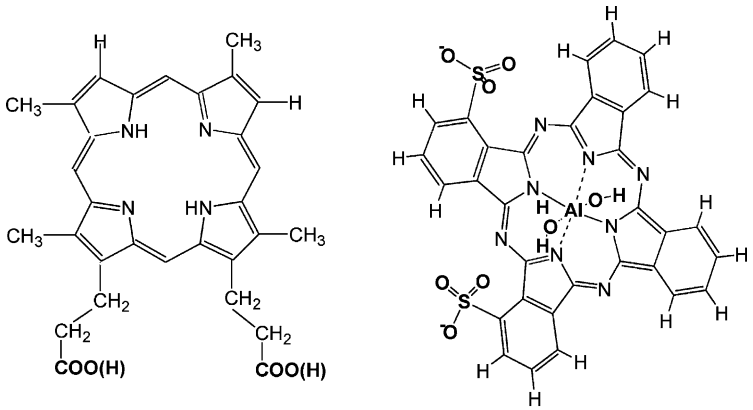

Fig. 1. Structures of deuteroporphyrin (a) and disulfonated aluminum phthalocyanine (b).

after the preparation of the solutions under study. Data thus obtained were treated as described elsewhere [18,20,29].

2.3. Dynamics of the interactions

Fast kinetics measurements were performed using an Applied Photophysics (Leatherhead, UK) stopped-flow apparatus with mixing time of 1.2 ms. The excitation light provided by the 150 W xenon arc lamp was passed through a monochromator with slits generally set to give a bandwidth of 4.65 nm. Fluorescence emission was collected above 590 nm using a low-cut filter (Oriel, France). The fluorescence signal was fed on a RISC workstation (Acorn Computers, UK). At least five traces were averaged for each experiment. Analysis of data was carried out by using the software provided by the manufacturer. It was based on the non-linear curve fitting Marquard algorithm that also provides uncertainties on the parameters obtained.

Steady state and dynamic measurements were performed at 25 °C in phosphate buffer saline, pH 7.4.

2.4. Microscopy equipment

The instrumental set-up was based on a Nikon Eclipse TE 300 DV inverted microscope equipped with a high numerical aperture phase oil objective (CFI Plan apochromat DM 60× n.a.: 1.4, Nikon France). An Osram HBO 100 W mercury lamp was used for fluorescence excitation. The mercury rays were isolated with narrow band interference filters mounted on a filter wheel positioned along the excitation path (λ 10-2, Sutter Instrument Company). Neutral density filters (ND × 8) were used to reduce excitation level. Image acquisition (1000 ms integration time) was performed with a back illuminated cooled detector (CCD EEV, NTE/CCD-1024-EB target with unichrome coating and ST-133 controller, 16 bit depth at 100 khz or 1 Mhz digitization rate, Roper Scientific, France). The detector was placed on the lateral video port of the microscope in conjunction with a 2.25× magnification relay lens). Data acquisition, processing and analysis were performed with Metamorph software, supplied by Universal Imaging Corporation (Roper Scientific, France).

2.5. Cell culture and experiments

Cells from the human fibroblast cell line HS68 were grown at 37 °C in DMEM (Dulbecco's Minimum Eagle Medium) supplemented with 10% fetal calf serum (FCS) and 100 U/mol Penicillin/Streptomycin. The incubator was filled with a humidified atmosphere of air and 5% CO_2. The cells were passaged every 6 days and used between the 13th and the 19th passages.

2.5.1. Microscopy experiments

Two days before experiments, the cells were seeded at 10000 cells/ml on a 0.17 mm thick cover glass. Then, the cover glass was washed with Hank's balanced salt solution (HBSS) and the cells incubated with the photosensitizer in the same medium for 15 min at 37 °C. For the first experiment series, the photosensitizers were used alone. Their concentrations were adjusted to [DP] = 2.5×10^{-7} M and [AlPcS2a] = 1×10^{-6} M. The higher concentration of the phthalocyanine compensates its lower fluorescence. In a second experiment series, the photosensitizers were first incubated with 1×10^{-7} M LDL for 15 min. As inferred from the kinetics experiments described in the result section, this time is more than sufficient to achieve loading of LDL with the photosensitizers. Then, the cells were incubated with these solutions for 15 min at 37 °C as before. A third series, used as control, involved experiments carried out by using the same protocol but without photosensitizer. In all cases, after incubation, the cells were washed twice with HBSS.

2.5.2. Subcellular localization

After cell treatments, the red fluorescence emission of the photosensitizers was collected through a bandpass filter (645 ± 75 nm, Omega). A bandpass filter (330–380 nm and a dichroic mirror at 400 nm were used for excitation. This wavelength range was chosen for all the experiments. It was found to provide sufficient emission signals for photosensitizers as well as for the organelle-specific probe LysoTracker® green (Molecular Probes). This makes it possible to excite the photosensitizer and the organelle probe without changing the excitation set-up, minimizing the delay between fluorescence image acquisitions.

LysoTracker® green was used to check lysosomal localization of AlPcS2a. Before incubation with the photosensitizer, the samples were washed twice and incubated 30 min with LysoTracker® green (200 nM). A bandpass filter (535 ± 45 nm, Omega) was used to isolate the green fluorescence emission of the probe. The emission wavelengths of phthalocyanine and LysoTracker® green were different enough to allow their successive characterization by using green and red bandpass filters, respectively. It can be mentioned that the fluorescence emission band of LysoTracker® green falls in a region without significant absorption of AlPcS2a. This makes unlikely any non-radiative energy transfer from the organelle probe to the phthalocyanine in colocalization experiments.

2.5.3. Quantification of photosensitizer uptake

Twenty-four hours before the experiment, HS68 were seeded at a density of 14,000 cells/cm^2 in 35 mm Petri dishes. The cells were used at about 70–80% of confluence. After washing with HBSS, cells were incubated for 15 min with 1 ml of either 2.5×10^{-7} M DP or 1×10^{-6} M AlPcS2a solubilized in HBSS or preloaded in 1×10^{-7} M LDL in HBSS. After incubation, cells were twice washed with 1 ml of HBSS and then scrapped in 900 μl of pure water leading to cell lysis. The disrupted cell solution was collected and added with 100 μl of a 3% Triton X-100

aqueous solution. Then, 150 μl were saved for protein determination according to the method of Lowry [30]. The remaining solution was used for the fluorimetric measurement of DP or AlPcS2a concentrations (λ_{exc} = 396 and 375 nm, λ_{em} = 621 and 675 nm, respectively). Solutions of known photosensitizer concentrations were used as standards. Data, expressed as μmol of DP or AlPcS2a per gram of protein, are the mean (± S.D.) of experiments performed in triplicate.

3. Results and discussion

3.1. Interactions of photosensitizers with membrane-models and LDL

In a first step, our aim was to fulfill the set of steady state and dynamic data available on the interactions of the photosensitizers with membranes and LDL, i.e. the major structures involved in the cellular transport of these molecules. The interaction of deuteroporphyrin with membrane-models has been thoroughly described in previous papers. This molecule possesses a high affinity for lipidic phosphatidylcholine unilamellar vesicles [29]. Owing to its asymmetrical structure, it localizes in each membrane leaflets with its polar carboxylic chains directed towards water interfaces (see Fig. 2). Both the entrance and the exit steps (see Fig. 2), characterized by the rate constants k_{on} and k_{off}, respectively, are extremely fast [29,31]. Although the transfer through the membrane bilayer (k_t) depends on the bilayer thickness [24] and cholesterol content [32], its rate can be assumed to be fast enough with regards to the duration of cellular experiments. Importantly, the rate of the transfer through the bilayer was found to drastically depend on pH leading to a strongly favored relocation from moderately acidic to neutral or slightly alkaline compartments [24,32]. The interaction of AlPcS2a with lipidic vesicles has been described elsewhere [33]. As for deuteroporphyrin, both the entrance and the exit steps from the outer hemileaflet of the vesicles were found to be very fast. The loss of a water molecule coordinated to the aluminum ion allows the molecule to penetrate somewhat deeper within the outer monolayer. The affinity of AlPcS2a for these membrane-models was also high, nearly 10 times higher than that of deuteroporphyrin. However, contrary to what observed for DP, kinetic experiments showed that the transfer across the membrane of AlPcS2a was extremely slow. Even for thin bilayers, it extends over hours [33]. Typical values for the half-reaction times characterizing these steps are reported in Table 1.

More recently, we studied the interactions of deuteroporphyrin with LDL under steady state and dynamic conditions [18]. We characterized binding sites near the apoprotein as well as incorporation of the molecules into the phospholipid outer layer of LDL (see Fig. 2). The overall affinity of DP for LDL was found to be very high

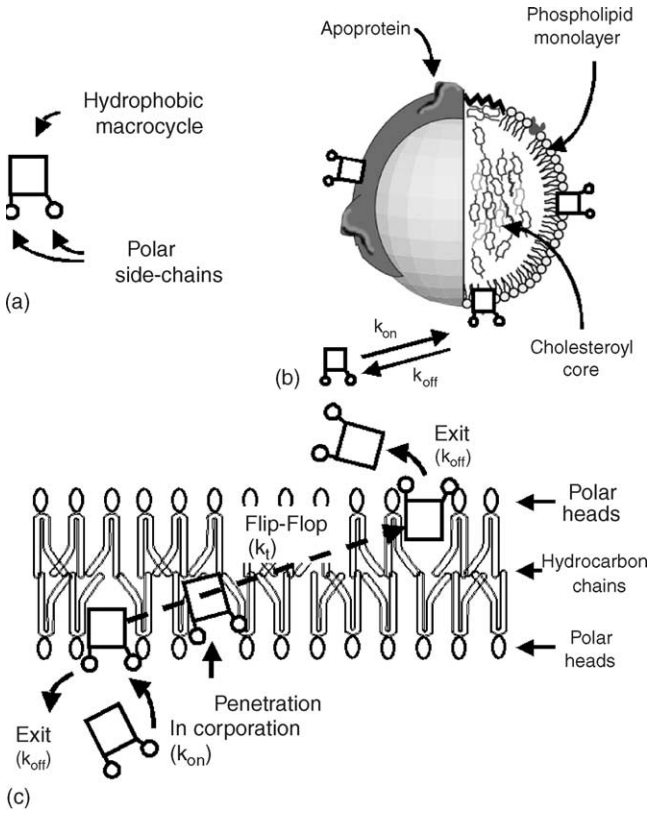

Fig. 2. (a) Basic structure of the amphiphilic photosensitizers used showing their common characteristic: a hydrophobic macrocycle bearing polar chains on one side. (b) Scheme of a low-density lipoprotein with potential binding sites for the amphiphilic macrocycles. The equilibrium with water-solubilized molecules involves the rate constants k_{on} and k_{off}. (c) Scheme of a membrane illustrating the steps involved in the passage of an amphiphilic macrocycle through a phospholipidic bilayer. The transfer is governed by the rate constant k_t. In this picture, the relative sizes of the macrocycle and the bilayer are respected.

($5.8 \times 10^8\ M^{-1}$). Importantly, the kinetics of the entrance and exit steps were found to be very fast, indicating that quick changes in the distribution of photosensitizers among LDL, various carriers and bulk medium could arise before LDL endocytose takes place.

Here, we report on the association of AlPcS2a to LDL in order to supplement the set of data available for the two molecules considered.

3.1.1. Steady state interactions of AlPcS2a with LDL

The fluorescence emission spectra of AlPcS2a (1.75×10^{-7} M) in PBS and in presence of various LDL concentrations (0, 1, 1.5, 2, 3, 4, 5 and 10×10^{-8} M) are given in Fig. 3. The excitation wavelength was 375 nm. Upon LDL addition the intensity of the fluorescence emission is increased significantly and slightly shifted from 677 to 674 nm. Similar changes were recorded upon binding of AlPcS2a to lipidic vesicles [33]. The plot of the fluorescence intensity versus the LDL concentration shows some leveling off (see Fig. 4a). However, screen effects limited the range of usable LDL concentrations. The value of the plateau is best obtained from an inverse plot (see Fig. 4b).

Table 1
Steady state and dynamics data for the interactions of DP and AlPcS2a with membrane-models and LDL

	Membrane-models			LDL		
	K_{ass}	t_{off}	t_t	K_{ass}	t_{on}	t_{off}
DP	$(1.4 \pm 0.2) \times 10^5\ M^{-1}$	32 ± 2 ms	1700 ± 500 ms	$(5.8 \pm 1.2) \times 10^8\ M^{-1}$	3.5 ± 0.2 ms; 2.3 ± 0.1 ms	120 ± 20 ms; 46 ± 9 ms
AlPcS2a	$(2.7 \pm 0.4) \times 10^6\ M^{-1}$	~0.2 s	Hours	$(5 \pm 1) \times 10^7\ M^{-1}$	0.14 ± 0.02 s; 0.2 ± 0.03 s	0.86 ± 0.08 s; 0.1 ± 0.01 s

The data for membrane-models correspond to the values obtained with dimyristoylphosphatidylcholine small unilamellar vesicles as reported in references [29] and [33] for DP and AlPcS2a, respectively. K_{ass} are overall association constants. The values of K_{ass} for the vesicles are expressed in terms of phospholipids. In order to compare these values to the K_{ass} values obtained with LDL, they should be multiplied by about 800, i.e. the number of phospholipids covering LDL. Data for the interactions between DP and LDL are taken from [18]. The characteristic half times, t_{off} and t_t, were computed as $0.693/k_{off}$ and $0.693/k_t$ in agreement with the exponential character of these processes. The values for the interactions of AlPcS2a with LDL were obtained in the present study. The values for t_{on} correspond to the LDL concentration used for cell experiments (1×10^{-7} M). When biphasic interactions were observed, data for both steps are given.

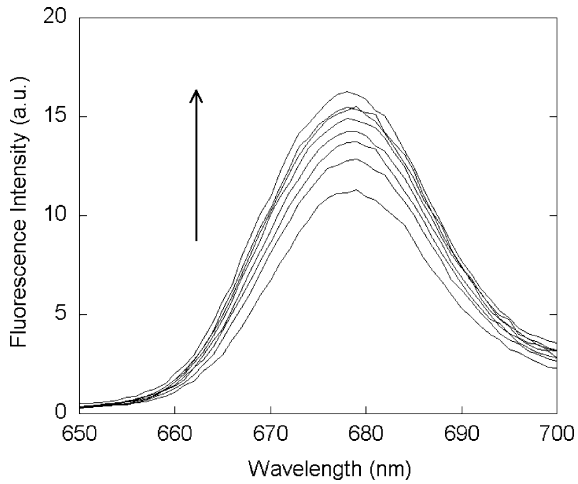

Fig. 3. Emission spectra of AlPcS2a (1.75×10^{-7} M) in buffer and in the presence of LDL (0, 1, 1.5, 2, 3, 4, 5, 10×10^{-8} M). The arrow indicates increasing LDL concentrations. The excitation wavelength was set at 375 nm.

This value is reported in Fig. 4a as a dashed line. The intercept between the plateau value and the initial slope of the curve shown in Fig. 4a corresponds to a LDL concentration of about 3×10^{-8} M. This indicates that each lipoprotein could bind about six phthalocyanine molecules at best. The half-plateau value was reached for a LDL concentration of about 2×10^{-8} M, which corresponds to an overall association constant around 5×10^7 M. Duplication of experiments with other sets of phthalocyanine and LDL concentrations led to consistent values for this

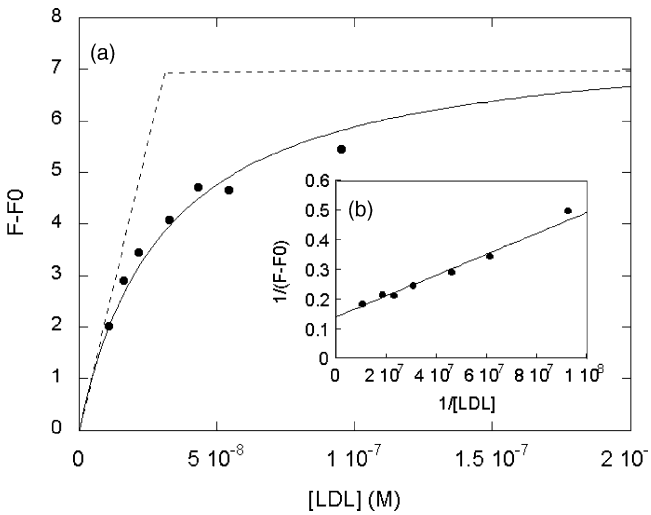

Fig. 4. Fluorescence changes of AlPcS2a (1.75×10^{-7} M) in presence of increasing concentrations of LDL. (a) Direct plot. The horizontal dashed line corresponds to the value extrapolated from the inverse plot shown in (b) for large LDL concentrations. The other dashed line corresponds to the initial slope of the curve. The two lines intercept for a LDL concentration of about 3×10^{-8} M. The maximum capacity of LDL to bind phthalocyanine is the ratio between AlPcS2a concentration and this value, i.e. about six molecules. (b) Inverse plot. F and F_0 are the fluorescence emission intensities of AlPcS2a at 675 nm with and without LDL, respectively. Excitation was set at 375 nm.

association constant. Analysis of data according to fully developed equations as we reported elsewhere [20,29] was not feasible however. Indeed, these procedures required that the amount of free sites on lipoproteins largely exceed that of occupied sites. These conditions would have been fulfilled through the use of smaller phthalocyanine concentrations. However, this possibility is limited because of the poor fluorescence of phthalocyanines.

3.1.2. Kinetic measurements

In stopped-flow experiments we measured signals that can be more easily amplified and averaged. Furthermore, attention was given on rates rather than on amplitudes. These measurements are less subjected to sensitivity problems and screen effects than those performed in steady state conditions.

In a first series of experiments, we mixed an AlPcS2a solution (4.4×10^{-8} M after mixing) with various LDL solutions (final concentrations 0.5, 0.75, 1, 1.25, 1.5 $\times$ 10^{-7} M) in the stopped-flow apparatus and fluorescence changes were recorded upon time. A typical signal is shown in Fig. 5a. In these experiments the binding capacity of the LDL greatly exceeds the number of bound molecules. Consequently, the kinetics of the interactions of AlPcS2a with LDL was considered to obey pseudo-first order conditions. The signal was nicely fitted by a biexponential curve (see Fig. 5b). This suggests that two different localizations of the phthalocyanine were involved, in keeping with results obtained with deuteroporphyrin. The binding process was fairly fast. At the LDL concentration (1×10^{-7} M) used for the cellular studies reported below, the half times corresponding to the two exponential steps are 0.14 $\pm$ 0.02 and 0.2 $\pm$ 0.03 s, respectively.

The rate of release of AlPcS2a from LDL was measured according to the well-described procedure of transfer to albumin [18,24,29,33]. The lipoproteins (7.5×10^{-8} M) were preloaded with AlPcS2a (2.2×10^{-8} M). This solution was mixed with albumin (1×10^{-4} M) that possess a good affinity for AlPcS2a [34]. Owing to the presence of albumin in large excess, equilibriums are strongly shifted towards binding to this protein. Assuming that the transfer occurs through the aqueous phase, the kinetics give access to the exit rate constants. A detailed analysis of the method was reported before [18]. As shown in Fig. 5c,d, a biexponential signal was recorded. Rate constants of 6.8 $\pm$ 0.7 and 0.8 $\pm$ 0.1 s^{-1} were obtained from the fit. They can be attributed to release of the phthalocyanine from two types of sites on LDL, in agreement with results obtained for the entrance process. The half times corresponding to the two release steps are given in Table 1. Again, it can be pointed out that they are extremely short.

3.2. Cellular experiments

3.2.1. Cell incorporation of deuteroporphyrin

After 15 min incubation of HS68 fibroblasts with a deuteroporphyrin solution, the fluorescence of the porphyrin is found to be relatively diffuse, suggesting membrane and cytosolic incorporation (Fig. 6a). A network structure suggestive of mitochondria appears to be more intensely labeled. No fluorescence was found in the

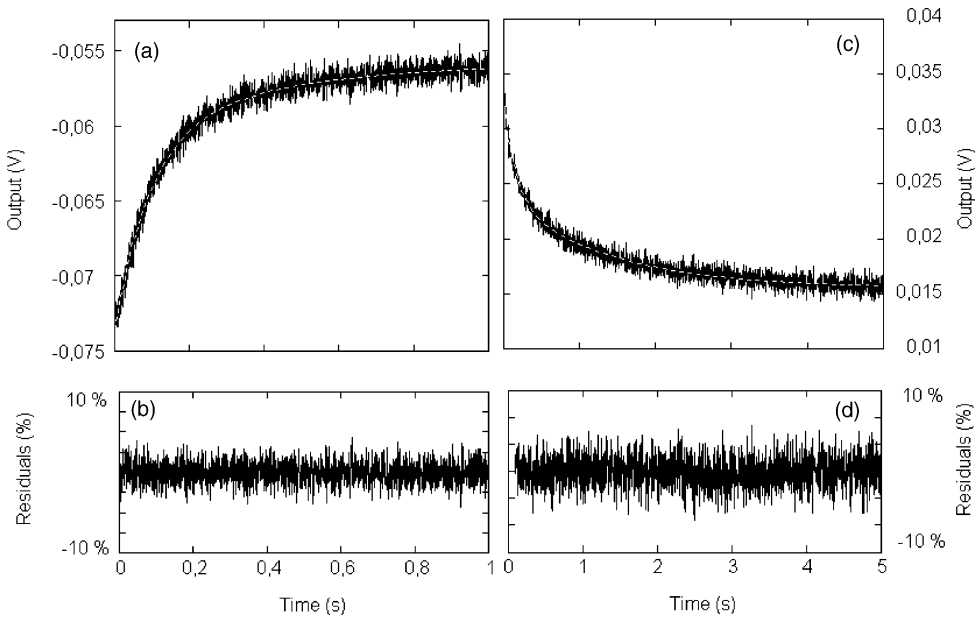

Fig. 5. Dynamics of the interactions of AlPcS2a with LDL. (a) Fluorescence changes accompanying the association of AlPcS2a (4.4×10^{-8} M) to LDL (1×10^{-7} M). (b) Residuals from a biexponential fit of the signal shown in (a). (c) Fluorescence changes accompanying the transfer of AlPcS2a pre-incubated with LDL towards albumin in excess (1×10^{-4} M). The rate of transfer is limited by the release of the phthalocyanine bound to LDL into the aqueous solution (see text). (d) Residuals from a biexponential fit of the signal shown in (c). Excitation wavelength: 375 nm.

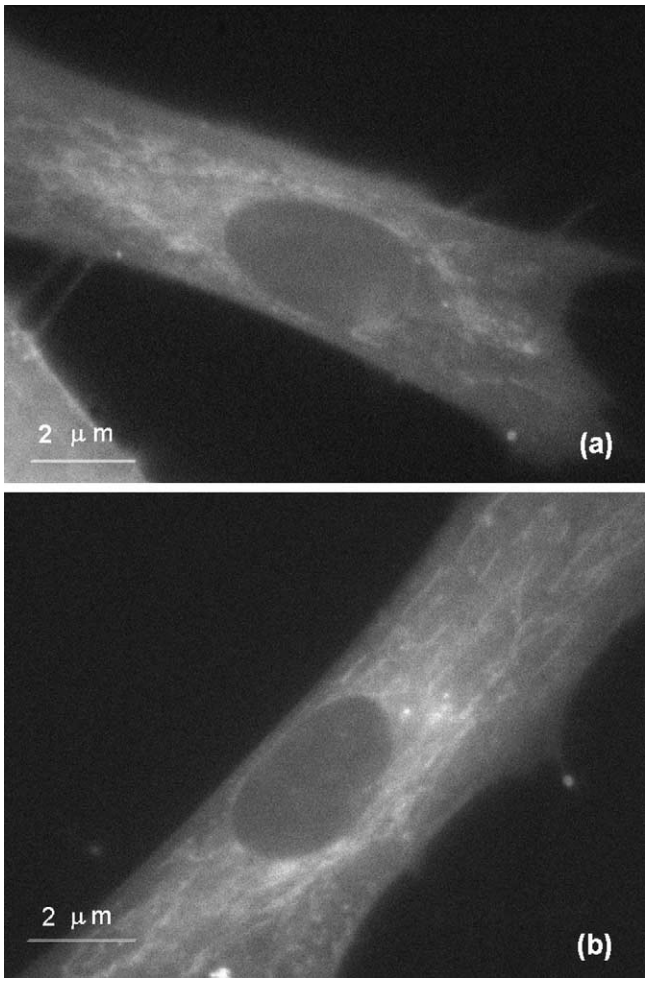

Fig. 6. Fluorescence microscopy study of the incorporation of DP into HS68 fibroblasts (excitation: 330–380 nm; emission: 645 ± 75 nm). (a) Cells incubated with DP alone (2.5×10^{-7} M) for 15 min. Fluorescence intensity range among the cell: 0–310 cps (counts per second). (b) Cells incubated with DP (2.5×10^{-7} M) pre-associated to LDL (1×10^{-7} M). Fluorescence intensity range among the cell: 0–160 cps.

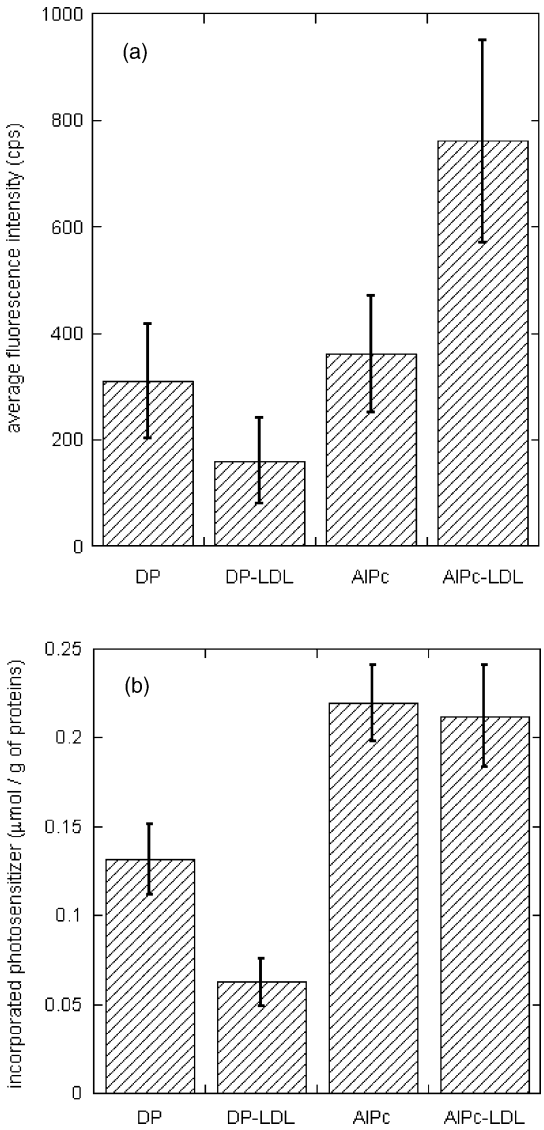

Fig. 7. Quantification of the effect of LDL on the cell incorporation of DP and AlPcS2a. (a) Fluorescence microscopy. Ten areas of 0.25 μm^2 in sites labeled by the photosensitizer were delimited on each cellular view. Each cell was credited with the average fluorescence intensity (expressed as counts per second, cps) measured on these areas. For each of the experimental conditions shown in the figure, 10 different cells were considered to determine a mean intensity and its standard error. The concentrations were the following: [DP] = 2.5×10^{-7} M; [AlPcS2a] = 1×10^{-6} M; [LDL] = 0 or 1×10^{-7} M. Excitation: 330–380 nm; emission: 645 ± 75 nm. (b) Extraction experiments. The amount of photosensitizer incorporated by cells is determined by fluorescence measurements on the extracts as described in the text. Data are normalized to the cellular protein content. The concentrations of photosensitizers and LDL were the same as in (a).

nucleus. The distribution of the porphyrin was not modified upon vectorization by lipoproteins (see Fig. 6b). The average fluorescence intensity of the cells incubated with deuteroporphyrin bound to LDL (DP–LDL) was around 160 cps (count per second) whereas that of cells incubated with the porphyrin alone (DP) was around 310 cps (Fig. 7a). Then, the cellular incorporation of the porphyrin in the presence of LDL is somewhat lower. This result was further confirmed by porphyrin extraction as shown in Fig. 7b.

Taken together these results indicate that LDL's have only a marginal effect on cell incorporation and subcellular localization of deuteroporphyrin even if the porphyrin is initially bound to the lipoproteins. This result can be easily explained by considering the dynamics of the interactions involved. The exchanges of DP molecules between the lipoproteins and the bulk incubation medium and between this medium and the plasma membrane of cells are very fast. As the transfer through the bilayer is also expected to be fast as shown by experiments on model systems, the porphyrin molecules associated with the plasma membrane are likely to quickly enter the cells by passive diffusion. Then, they will distribute in other membrane structures within the cells. As a consequence, the binding equilibrium between LDL and porphyrins will be quickly displaced toward cellular incorporation, the internal membranes providing a very large number of accessible sites. Furthermore, even if deuteroporphyrin molecules do enter within

cells by LDL-mediated endocytose, they will reach endosomes and lysosomes from which they will escape. It must be pointed out that release of carboxylic porphyrins from the acidic endosomal/lysosomal compartment is strongly favored due to the pH gradient between these organelles and the cytoplasm [32,35]. Finally, it should be noted that some porphyrins could remain associated with lipoproteins outside the cells. This would explain why the porphyrin uptake in the absence of LDL was a little more important than that obtained with LDL. Thus, the incorporation and cellular distribution of deuteroporphyrin within fibroblasts is fully consistent with the dynamics of interaction of this molecule with LDL and membrane-models in acellular systems. Obviously, the intracellular pattern distribution may depend on the cell line and/or the incubation protocol. Intracellular deuteroporphyrin distribution within lymphoblasts was found to be somewhat different to that reported here [36]. But in keeping with previous studies on lymphoblast lines [37], these differences are not in contradiction with a major role of passive transfer through membranes.

3.2.2. *Cell incorporation of disulfonated aluminum phthalocyanine*

As shown in Fig. 8a, when cells were incubated with AlPcS2a in the absence of LDL, this molecule was found to be mainly localized within intracellular vesicles. In order to better identify these vesicles, co-localization experiments were performed with a lysosome specific probe, LysoTracker® green. Images were taken with filters allowing the transmission of red and green light in order to monitor the fluorescence emission of the phthalocyanine and that of the lysosome probe, respectively. The superposition of red and green images shows little evidence for co-localization in this case. Most of the intracellular vesicles shown on this picture are not lysosomes. As noted in Table 1, the transfer of AlPcS2a through lipid bilayers is extremely slow, far beyond the time scale of our experiments. The uptake of AlPcS2a within cells by passive diffusion is very unlikely. Also, no re-distribution of the dye by passive transfer through internal membranes is expected within a short period of time. In the absence of lipoproteins, bulk endocytose is likely to mostly contribute to AlPcS2a incorporation. Possibly, the phthalocyanine did not reach lysosomes and was still localized into endosomes during this relatively short incubation time. However, this bulk endocytose process is efficient. It can be noted that the cells incorporate larger amount of AlPcS2a than DP on a quantitative basis (see Fig. 7b).

When incubation was carried out in the presence of LDL (Fig. 8b), the cells also exhibited intracellular red-fluorescent vesicles. However, as compared to experiments without LDL, the red fluorescence appeared more intense (760 cps against 160 cps, see Fig. 7a). Moreover, as shown by co-localization experiments, the nature of a large part of the vesicles is different. A significant overlap was found between the red fluorescence of the phthalocyanine and the green fluorescence of LysoTracker® indicating major localization of AlPcS2a in lysosomes. Thus, the incubation of cells with lipoprotein-associated AlPcS2a favors incorporation by LDL-mediated endocytose, which brings the phthalocyanine into lysosomes. However, as shown in Fig. 7b, the overall uptake of AlPcS2a is not increased in the presence of LDL. In fact, non-mediated endocytose of AlPcS2a from the incubation solution appears as a fairly efficient process. Association to lipoproteins hampers this pathway. It can be expected that LDL-mediated endocytose

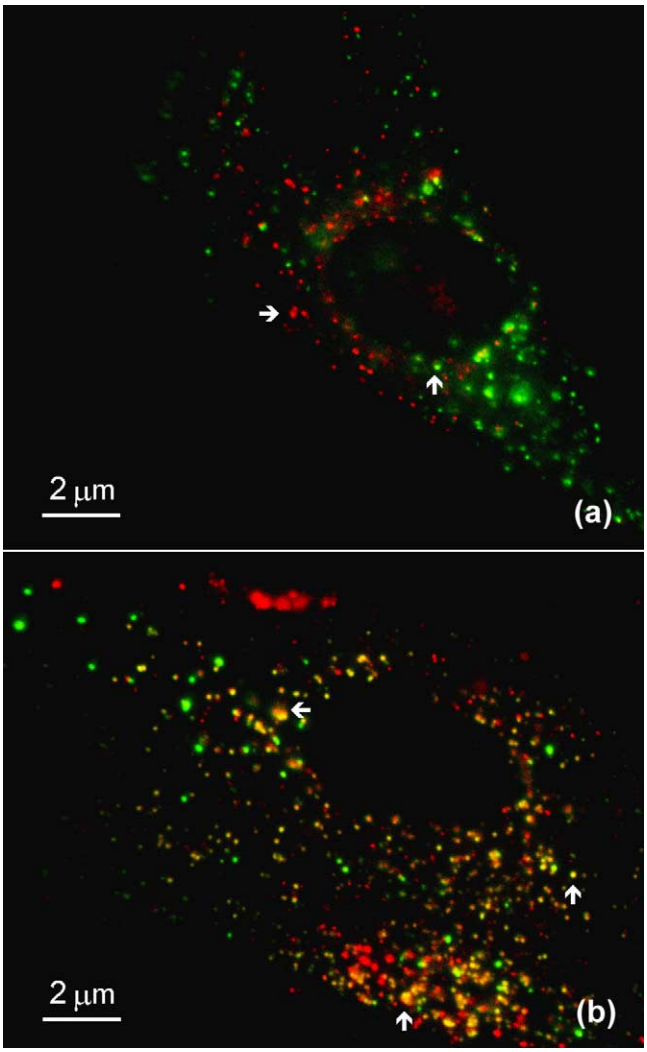

Fig. 8. Fluorescence microscopy study of the incorporation of AlPcS2a into HS68 fibroblasts (a) Cells incubated with AlPcS2a (1×10^{-6} M) alone for 15 min. Fluorescence intensity range among the cell: 0–360 cps (counts per second). (b) Cells incubated with AlPcS2a (1×10^{-6} M) pre-associated to LDL (1×10^{-7} M). Fluorescence intensity range among the cell: 0–760 cps. In both cases, cells were pre-labeled with LysoTracker® green (2×10^{-7} M). Fluorescence excitation: 330–380 nm. The red AlPcS2a emission and the green LysoTracker® emission were collected by using filters at 645 ± 75 and 535 ± 45 nm, respectively. The overlays of green and red images are shown. When the phthalocyanine is associated to LDL (panel b), it localizes into lysosomes as illustrated by yellow spots resulting from the overlay of red and green emissions. In panel a, no or very little overlay can be seen. Arrows in each panel indicate typical spots.

just compensates this effect in the present experimental conditions. The increase of the fluorescence intensity observed for cells incubated with AlPcS2a associated to LDL (Fig. 7a) is somewhat misleading. However, it was previously observed that fluorescence quantum yield of AlPcS2a is sensitive to concentration effects [38]. Also, the interaction of AlPcS2a with membranes is affected by pH through protonation equilibria of ligands bound to the aluminium ion [33]. These features make difficult a comparison of the two images shown in Fig. 8 on a quantitative basis.

Granular fluorescence pattern and lysosome localization of sulfonated phthalocyanines or porphyrins have been observed for various cell lines [39,40] in agreement with their inability to cross membrane rapidly. The uptake of non-sulfonated zinc phthalocyanine and its tetrasulfonated derivative in absence or presence of LDL has been reported [41]. The first compound required liposomal formulation due to its high hydrophobicity. The transfer of the photosensitizer from liposomes to lipoproteins is likely to be important [42,43] and under the control of dynamics parameters similar to those investigated here. In a general way, the balance between amphiphilic and hydrophobic properties of photosensitizers was found to determine the extent of their LDL-mediated uptake [44].

The subcellular localization of photosensitizers is a major determinant of their efficacy. It has been noted that a diffuse cytoplasmic distribution may be a good prognostic for photodynamic activity [12]. Besides, the retention of photosensitizers such as AlPcS2a in the endosomal/lysosomal compartment is used in a new technology, named photochemical internalization (PCI). In this approach photochemical reactions in non-lethal conditions lead to rupture of endocytic vesicles favoring access of macromolecules (proteins, nucleic acids) to their targets localized in the cytoplasm or the nucleus [45,46].

To conclude, the present results give new insight into the mechanisms of cellular uptake of lipophilic and amphiphilic drugs and might reconcile some contradictive observations on the role of lipoproteins [19]. The knowledge of the dynamics of interactions of the drugs with LDL and membranes appears to be essential to understand how they could be targeted towards pathological growing tissues. The subcellular localization is under control of the kinetics of drug-membrane interactions. The appraisal of these dynamics factors will help in the design of new photosensitizers and delivery systems.

Acknowledgements

The authors thank Prof. David Phillips (Imperial College of Science, London) for a generous gift of the disulfonated aluminium phthalocyanine and Dr. Christine Vever-Bizet for her kind support during this work. Fluorescence microscopy experiments were performed by using the apparatus installed at CEMIM, a division of the National Museum of Natural History (MNHN) under the guidance of Dr. Marc Gèze and Dr. Marc Dellinger. We particularly thank Josiane Haigle for her skillful help in cellular experiments. The charity associations ARC and RETINA supported this work through PhD grants to S.B. The stopped-flow apparatus was acquired thanks to subsidy from ARC (grant # 7209).

References

[1] Levy JG, Obochi M. New applications in photodynamic therapy. Introduction. Photochem Photobiol 1996;64:737–9.
[2] Ackroyd R, Kelty C, Brown N, Reed M. The history of photodetection and photodynamic therapy. Photochem Photobiol 2001;74:656–69.
[3] Ochsner M. Photophysical and photobiological processes in the photodynamic therapy of tumours. J Photochem Photobiol B 1997;39:1–18.
[4] Piette J, Volanti C, Vantieghem A, Matroule JY, Habraken Y, Agostinis P. Cell death and growth arrest in response to photodynamic therapy with membrane-bound photosensitizers. Biochem Pharmacol 2003;66:1651–9.
[5] Woodburn KW, Vardaxis NJ, Hill JS, Kaye AH, Reiss JA, Phillips DR. Evaluation of porphyrin characteristics required for photodynamic therapy. Photochem Photobiol 1992;55:697–704.
[6] Dellinger M. Apoptosis or necrosis following Photofrin photosensitization: influence of the incubation protocol. Photochem Photobiol 1996;64:182–7.
[7] Kessel D, Luo Y, Deng Y, Chang CK. The role of subcellular localization in initiation of apoptosis by photodynamic therapy. Photochem Photobiol 1997;65:422–6.
[8] Hsieh YJ, Wu CC, Chang CJ, Yu JS. Subcellular localization of Photofrin determines the death phenotype of human epidermoid carcinoma A431 cells triggered by photodynamic therapy: when plasma membranes are the main targets. J Cell Physiol 2003;194:363–75.
[9] Berg K, Bommer JC, Winkelman JW, Moan J. Cellular uptake and relative efficiency in cell inactivation by photoactivated sulfonated meso-tetraphenylporphines. Photochem Photobiol 1990;52:775–81.
[10] Boyle RW, Dolphin D. Structure and biodistribution relationships of photodynamic sensitizers. Photochem Photobiol 1996;64:469–85.
[11] MacDonald IJ, Morgan J, Bellnier DA, Paszkiewicz GM, Whitaker JE, Litchfield DJ, et al. Subcellular localization patterns and their relationship to photodynamic activity of pyropheophorbide-a derivatives. Photochem Photobiol 1999;70:789–97.
[12] Ball DJ, Mayhew S, Wood SR, Griffiths J, Vernon DI, Brown SB. A comparative study of the cellular uptake and photodynamic efficacy of three novel zinc phthalocyanines of differing charge. Photochem Photobiol 1999;69:390–6.
[13] Gal D, Ohashi M, MacDonald PC, Buchsbaum HJ, Simpson ER. Low-density lipoprotein as a potential vehicle for chemotherapeutic agents and radionucleotides in the management of gynecologic neoplasms. Am J Obstet Gynecol 1981;139:877–85.
[14] Vitols S, Peterson C, Larsson O, Holm P, Aberg B. Elevated uptake of low density lipoproteins by human lung cancer tissue in vivo. Cancer Res 1992;52:6244–7.
[15] Jori G, Beltramini M, Reddi E, Salvato B, Pagnan A, Ziron L, et al. Evidence for a major role of plasma lipoproteins as hematoporphyrin carriers in vivo. Cancer Lett 1984;24:291–7.
[16] Reyftmann JP, Morliere P, Goldstein S, Santus R, Dubertret L, Lagrange D. Interaction of human serum low density lipoproteins with porphyrins: a spectroscopic and photochemical study. Photochem Photobiol 1984;40:721–9.

[17] Kessel D. Porphyrin-lipoprotein association as a factor in porphyrin localization. Cancer Lett 1986;33:183–8.
[18] Bonneau S, Vever-Bizet C, Morlière P, Mazière JC, Brault D. Equilibrium and kinetic studies of the interactions of a porphyrin with low density lipoproteins. Biophys J 2002;83:3470–81.
[19] Kongshaug M, Moan J, Brown SB. The distribution of porphyrins with different tumour localising ability among human plasma proteins. Br J Cancer 1989;59:184–8.
[20] Brault D, Vever-Bizet C, Le Doan T. Spectrofluorimetric study of porphyrin incorporation into membrane-models: evidence for pH effects. Biochim Biophys Acta 1986;857:238–50.
[21] Brault D. Physical–chemistry of porphyrins and their interactions with membranes. The importance of pH. J Photochem Photobiol B 1990;6:79–86.
[22] Barrett AJ, Kennedy JC, Jones RA, Nadeau P, Pottier RH. The effect of tissue and cellular pH on the selective biodistribution of porphyrin-type photochemotherapeutic agents: a volumetric titration study. J Photochem Photobiol B 1990;6:309–23.
[23] Pottier R, Kennedy JC. The possible role of ionic species in selective biodistribution of photochemotherapeutic agents toward neoplastic tissue. J Photochem Photobiol B 1990;8:1–16.
[24] Maman N, Brault D. Kinetics of the interactions of a dicarboxylic porphyrin with unilamellar lipidic vesicles: interplay between bilayer thickness and pH in rate control. Biochim Biophys Acta 1998;1414: 31–42.
[25] Peng Q, Moan J, Nesland JM, Rimington C. Aluminum phthalocyanines with asymmetrical lower sulfonation and with symmetrical higher sulfonation: a comparison of localizing and photosensitizing mechanism in human tumor LOX xenografts. Int J Cancer 1990;46: 719–26.
[26] Chan WS, Svensen R, Phillips D, Hart IR. Cell uptake, distribution and response to aluminium chloro sulphonated phthalocyanine, a potential anti-tumour photosensitizer. Br J Cancer 1986;53:255–63.
[27] Ambroz M, Beeby A, MacRobert AJ, Simpson MS, Svensen RK, Phillips D. Preparative analytical and fluorescence spectroscopic studies of sulphonated aluminium phthalocyanine photosensitizers. J Photochem Photobiol B 1991;9:87–95.
[28] Bishop SM, Khoo BJ, MacRobert AJ, Simpson MS, Phillips D, Beeby A. Characterisation of the photochemotherapeutic agent disulphonated aluminium phthalocyanine and its high-performance liquid chromatographic separated components. J Chromatogr 1993;646: 345–50.
[29] Kuzelova K, Brault D. Kinetic and equilibrium studies of porphyrin interactions with unilamellar lipidic vesicles. Biochemistry 1994;33: 9447–59.
[30] Lowry OM, Rosebrough NJ, Farr AL, Randall RJ. Protein measurement with the Folin phenol reagent. J Biol Chem 1955;193:265–75.
[31] Vever-Bizet C, Brault D. Kinetics of incorporation of porphyrins into small unilamellar vesicles. Biochim Biophys Acta 1993;1153:170–4.
[32] Kuzelova K, Brault D. Interactions of dicarboxylic porphyrins with unilamellar lipidic vesicles: drastic effects of pH and cholesterol on kinetics. Biochemistry 1995;34:11245–55.
[33] Maman N, Dhami S, Phillips D, Brault D. Kinetic and equilibrium studies of incorporation of di-sulfonated aluminum phthalocyanine into unilamellar vesicles. Biochim Biophys Acta 1999;1420: 168–78.
[34] Ambroz M, MacRobert AJ, Morgan J, Rumbles G, Foley MSC. Phillips D. Time-resolved fluorescence spectroscopy and intracellular imaging of disulphonated aluminium phthalocyanine. J Photochem Photobiol B 1994;22:105–17.
[35] Bonneau S, Maman N, Brault D. Dynamics of pH-dependent self-association and membrane binding of a dicarboxylic porphyrin: a study with small unilamellar vesicles. Biochim Biophys Acta 2004;1661:87–96.
[36] Ouedraogo GD, Redmond RW. Secondary reactive oxygen species extend the range of photosensitization effects in cells: DNA damage produced via initial membrane photosensitization. Photochem Photobiol 2003;77:192–203.
[37] Dellinger M, Vever-Bizet C, Brault D, Delgado O, Rosenfeld C. Cellular uptake of hydroxyethylvinyldeuteroporphyrin (HVD) and photoinactivation of cultivated human leukemia (REH6) cells. Photochem Photobiol 1986;43:639–47.
[38] Dhami S, Rumbles G, MacRobert AJ, Phillips D. Comparative photophysical study of disulfonated aluminum phthalocyanine in unilamellar vesicles and leukemic K562 cells. Photochem Photobiol 1997;65:85–90.
[39] Moan J, Berg K, Anholt H, Madslien K. Sulfonated aluminium phthalocyanines as sensitizers for photochemotherapy. Effects of small light doses on localization, dye fluorescence and photosensitivity in V79 cells. Int J Cancer 1994;58:865–70.
[40] Wessels JM, Strauss W, Seidlitz HK, Ruck A, Schneckenburger H. Intracellular localization of meso-tetraphenylporphine tetrasulphonate probed by time-resolved and microscopic fluorescence spectroscopy. J Photochem Photobiol B 1992;12:275–84.
[41] Valduga G, Bianco G, Csik G, Reddi E, Masiero L, Garbisa S, et al. Interaction of hydro- or lipophilic phthalocyanines with cells of different metastatic potential. Biochem Pharmacol 1996;51: 585–90.
[42] Ginevra F, Biffanti S, Pagnan A, Biolo R, Reddi E, Jori G. Delivery of the tumour photosensitizer zinc(II)-phthalocyanine to serum proteins by different liposomes: studies in vitro and in vivo. Cancer Lett 1990;49:59–65.
[43] Jori G, Reddi E. The role of lipoproteins in the delivery of tumour-targeting photosensitizers. Int J Biochem 1993;25: 1369–75.
[44] Polo L, Valduga G, Jori G, Reddi E. Low-density lipoprotein receptors in the uptake of tumour photosensitizers by human and rat transformed fibroblasts. Int J Biochem Cell Biol 2002;34:10–23.
[45] Berg K, Selbo PK, Prasmickaite L, Tjelle TE, Sandvig K, Moan J, et al. Photochemical internalization: a novel technology for delivery of macromolecules into cytosol. Cancer Res 1999;59:1180–3.
[46] Hogset A, Prasmickaite L, Selbo PK, Hellum M, Engesaeter BB, Bonsted A, et al. Photochemical internalisation in drug and gene delivery. Adv Drug Deliv Rev 2004;56:95–115.